Maximum Likelihood Failure Detection Techniques Applied to the Shuttle RCS Jets

John J. Deyst* and James C. Deckert*
The Charles Stark Draper Laboratory, Inc., Cambridge, Mass.

A software technique for onboard detection and identification of hard failures and leaks of the shuttle orbiter reaction control subsystem jets during the orbital flight phase is presented. The method uses only the gimbal angle and linear velocity measurements available from the orbiter inertial measurement unit. The system produces rotational state estimates required by the attitude autopilot in addition to performing failure identification. Uncoupled steady-state constant covariance extended Kalman filters with residual traps are employed for rotational and translational state estimation, and generalized likelihood ratio tests are made for failure identification. Rigid body simulation results indicate station-level identification times of less than 2 sec for primary jet hard failures and less than 70 sec for vernier jet hard failures and primary jet leaks.

Nomenclature

$\boldsymbol{a}$ = composite six-vector of angular and linear disturbing accelerations caused by jet failures
$\boldsymbol{a}_d$ = disturbing linear acceleration in principal body axes
$\boldsymbol{a}_J$ = linear acceleration caused by commanded jet firings
b_i = bias of IMU integrating accelerometer i
$\boldsymbol{c}_i$ = acceleration influence coefficient six-vector for jet station i
C_i = jet command component along IMU inertial axis i
$e_{b,i}$ = uncalibrated bias of accelerometer i
$\boldsymbol{e}_J$ = linear acceleration error caused by nominal jet firing inaccuracies
$\bar{e}_{m,i}$ = mean value of quantization error for accelerometer i
$E_{b,i}$ = variance of uncalibrated bias of accelerometer i
$\bar{E}_i$ = recursively calculated component of W_i
E_J = covariance of linear velocity error caused by $\boldsymbol{e}_J$ over one sample interval
$E_{\eta,i}$ = variance of linear velocity error along IMU inertial axis i caused by η_i over one sample interval
$E_{\mu,i}$ = variance of μ_i
f_i = force exerted by a failure at jet station i
H = measurement geometry row vector for general system
I_x, I_y, I_z = principal moments of inertia
$\ell(f_i^*)$ = likelihood argument for jet station i
m_i = output of accelerometer i
M = measurement history
$\hat{m}_x, \hat{m}_y, \hat{m}_z$ = commanded jet torques about principal axes
$N(q)$ = norm of quaternion q
$p(\boldsymbol{a}\,|M)$ = probability density function of $\boldsymbol{a}$ conditioned on M
P = estimation error covariance for general system
P_a = covariance of the error in the estimate of $\boldsymbol{a}$
P_d = covariance of error in the estimate of $\boldsymbol{a}_d$
P_ξ = estimation error covariance for ξ angular channel
q, q_j = quaternions
q_j^i = attitude quaternion representing the rotation of reference frame i to reference frame j
Q = IMU gimbal angle quantum size
Q_v = IMU integrating accelerometer quantum size
$Q\{\cdot\}$ = quantization operator
r = variance of the error in attitude measurement
R = scalar measurement error variance for general system
R_{Bi}^I = ith row of R_B^I, the direction cosine matrix transforming principal body axes to IMU inertial axes.
S = covariance of discrete process noise for angular channel
S_d = covariance of fictitious discrete process noise for linear disturbing acceleration estimator
t_n = discrete value of time
v_i = linear velocity component along IMU inertial axis i
$\boldsymbol{v}^j$ = fixed vector in reference frame j
W_i = variance of measurement error of accelerometer i
$\boldsymbol{x}$ = state vector for general system
y = scalar measurement for general system
$\alpha_{d,\xi}$ = component of vehicle disturbing angular acceleration along ξ axis
Δ = time step for discrete state estimator
$\tilde{\epsilon}$ = vector of small angle measurement residuals
η_i = process noise component along IMU axis i
λ_j = scalar component of quaternion j
μ_i = random component of quantization error of accelerometer i
$\tilde{\xi}$ = dummy variable assuming the symbols $\tilde{\phi}$, $\tilde{\theta}$, and $\tilde{\psi}$ to denote the components of $\tilde{\epsilon}$
ρ_j = vector component of quaternion j
ρ^+ = piecewise constant linear disturbing acceleration estimation error variance
Φ = state transition matrix for angular channel
ω_ξ = component of vehicle angular velocity along ξ axis

Subscripts

d = disturbing acceleration
x, y, z = principal body axes
ϕ, θ, ψ = roll, pitch, yaw axes, synonymous with motion about x, y, z axes respectively
ξ = dummy variable assuming the symbols ϕ, θ, and ψ to denote variables in the roll, pitch, and yaw channels respectively

Presented as Paper 75-155 at the AIAA 13th Aerospace Sciences Meeting, Pasadena, Calif., Jan. 20-22, 1975; submitted March 21, 1975; revision received Aug. 18, 1975. Work supported under Contract NAS9-13809 with the NASA Johnson Space Center.

Index categories: Navigation, Control, and Guidance Theory; Spacecraft Attitude Dynamics and Control.

*Staff Engineer, Control and Flight Dynamics Division. Member AIAA.

Superscripts

$\hat{}$	= estimated quantity
$\tilde{}$	= measured quantity or residual
+	= value immediately after discrete measurement incorporation
−	= mean value
*	= maximum likelihood estimate
′	= conjugate of quaternion

Reference frames

I	= IMU inertial frame
$\hat{B}$	= estimated body frame implied by estimated body attitude quaternion
$\hat{B}$	= measured body frame implied by measured body attitude quaternion

I. Introduction

THE space shuttle orbiter reaction control subsystem (RCS) consists of thirty-eight primary jets and six vernier jets located at fourteen stations on the vehicle. The current nominal thrust levels are 900 lb for the primary jets and 25 lb for the vernier jets. This paper addresses the problem of detecting and identifying the hard failure of a primary or vernier jet and the leaking of propellant of a primary jet during the orbital mission phase. This failure detection and identification (FDI) is accomplished using only the gimbal angle and the linear velocity measurements from the three onboard inertial measurement units (IMU's), and no additional hardware or measurements are required.

The evolution of methods and algorithms for effective FDI has progressed significantly in recent years. Work by Beard[1] and Jones[2] resulted in a systematic algebraic method for designing fault detection filters for linear stationary systems. Chien[3] exploited and extended the sequential probability ratio technique pioneered by Wald[4] to detect failures in navigation systems. Willsky, Deyst, and Crawford[5] adopted the bank of filters approach of Buxbaum and Haddad[6] to detection and compensation of jump failures. Mehra and Peschon,[7] and more recently Willsky and Jones,[8] exploited the characteristics of the innovations process of optimal estimation to develop efficient fault detection methods. The method developed in Ref. 9 and presented herein is a practical application of some of these methods to a specific FDI problem.

The FDI system makes use of generalized likelihood ratio (GLR) methods[10] and optimal estimation theory[11] to reliably identify failures and minimize false alarms. Accurate vehicle attitude and angular velocity estimates are developed as an integral part of the FDI system, and thus the system performs the task of vehicle attitude estimation as well as jet FDI. The estimators were developed originally under the assumption that estimation error covariances would be calculated in real time. Simulation of these estimators indicated that the error covariances were nearly constant [illegible]vely long periods of time. It was found that the determining factor was whether or not jets were firing. Hence the real time covariance calculation was subsequently eliminated, and piecewise constant covariances employed. Three sets of covariances were found to be adequate: one for coasting periods when no jets are firing, a second set when jets are being commanded to fire, and the third set for use in identifying a hard primary jet failure after it has been detected.

The FDI algorithm uses the current estimates of disturbing linear and angular acceleration to determine the maximum likelihood estimates of the forces due to jet leaks at each of the jet stations. GLR techniques are then employed using these maximum likelihood jet force estimates to determine which, if any, of the jet stations has failed.

II. System Modeling and Estimation

The ability to detect and identify jet failures from IMU data is strongly dependent upon the physical properties and geometry of the spacecraft. Figure 1 illustrates the station thrust directions for the FD-2 shuttle orbiter RCS jet configuration. Multiple jets at a particular station are separated from one another by approximately one foot. Because of the small differences in moment arm lengths for jets at the same station, compared to the expected thrust variations in an unfailed jet, and because the exact thrust to be expected from a leaky jet is not well known; no single jet failure may be distinguished dynamically from a similar failure of another jet at the same station. Therefore, this paper will only be concerned with the identification of jet station failures. However, it is not difficult to envision manual procedures utilizing selective jet firing and propellant enabling commands together with the output of the algorithm developed in this paper to identify individual failed jets.

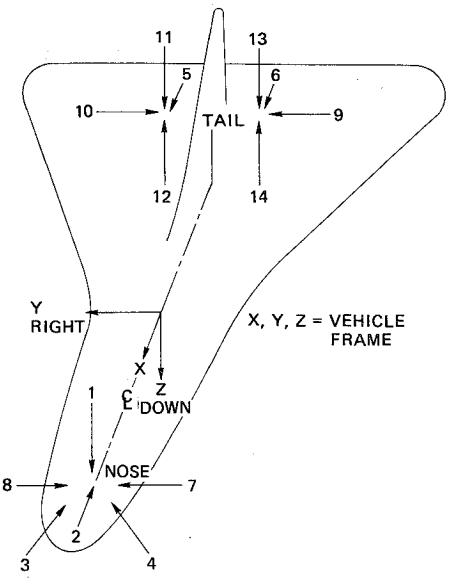

Fig. 1 Jet station locations and thrust directions.

In order to identify RCS jet station failures using IMU data, it is necessary to compute estimates of the disturbing angular acceleration and linear acceleration of the shuttle orbiter, in body coordinates, arising from unexpected jet activity. These disturbing angular and linear accelerations are statistically correlated since they arise from the application of physical forces on the vehicle. Thus, to minimize estimation error, these variables should be estimated together to exploit the information contained in the correlation. However, the dimensionality and corresponding computational requirements of the combined estimation of rotational and translational state variables precludes this approach in an onboard autopilot system. Additionally, the correlation between the rotational and translational state variables is not high, so neglecting the cross-correlations does not appreciably degrade estimator performance.

In the following two subsections, discrete time-varying estimators for rotational and translational state variables are developed which utilize only information available from the IMU. These estimators are subsequently simplified to employ piecewise constant covariances.

Rotational Estimation

Because of its reduced dimension and computational simplicity, the attitude quaternion was selected as the angular position state variable. The attitude quaternion is a four-dimensional representation of a rotation about a single axis.[12] The quaternion consists of a scalar and a vector part, with the notation

$$q = \lambda + \rho \tag{1}$$

The scalar portion represents the cosine of half the rotation angle, and the vector portion represents the sine of half the rotation angle times a unit vector along the axis of rotation u. The conjugate q' of the quaternion q in Eq. (1) is given by

$$q' = \lambda - \rho \tag{2}$$

The product of two quaternions is given by

$$q_1 q_2 = \lambda_1 \lambda_2 - \rho_1 \cdot \rho_2 + \lambda_1 \rho_2 + \lambda_2 \rho_1 \times \rho_2 \tag{3}$$

and the norm of a quaternion $N(q)$ is given by

$$N(q) = qq' = q'q = \lambda^2 + \rho \cdot \rho \tag{4}$$

It follows from Eqs. (1-4) that the norm of the attitude quaternion is one.

Define the attitude quaternion q_2^1 as the quaternion representing the single rotation through which reference frame 1 must be rotated to align with reference frame 2. The representation of a fixed vector in frame 1, v^1, is related to its representation in frame 2, v^2, by

$$v^1 = q_2^1 v^2 (q_2^1)' \tag{5}$$

where the vector in the above quaternion multiplication is treated as a quaternion with a zero scalar component. It then follows that

$$q_3^1 = q_2^1 \, q_3^2 \tag{6}$$

The attitude quaternion employed in this study is q_B^I, where I represents the inertial reference frame and B represents the shuttle orbiter principal axis frame. The principal axis frame is near the vehicle body frame, and roll, pitch, and yaw are defined as rotations about the x, y, and z principal axes respectively.

Between successive discrete IMU measurement times differing by the small time step Δ, the estimated quaternion in propagated by the second order equation[12]

$$q_{\hat{B}}^I(t_{n+1}) = q_{\hat{B}+}^I(t_n)\,[I - \hat{\omega}^+(t_n)\cdot\hat{\omega}^+(t_n)\Delta^2/8 + \{\hat{\omega}^+(t_n) + \hat{\omega}(t_{n+1})\}\Delta/4] \tag{7}$$

where the plus superscript indicates variables after measurement incorporation, the angular velocities in roll, pitch and yaw satisfy Euler's equations, and the estimated angular velocity components are thus propagated by the first order equations[13]

$$\hat{\omega}_\phi(t_{n+1}) = \hat{\omega}_\phi^+(t_n) + \left[\frac{I_y - I_z}{I_x}\hat{\omega}_\theta^+(t_n)\hat{\omega}_\psi^+(t_n) + \frac{\hat{M}_x(t_n)}{I_x} + \hat{\alpha}_{d,\phi}^+(t_n)\right]\Delta$$

$$\hat{\omega}_\theta(t_{n+1}) = \hat{\omega}_\theta^+(t_n) + \left[\frac{I_z - I_x}{I_y}\hat{\omega}_\phi^+(t_n)\hat{\omega}_\psi^+(t_n) + \frac{\hat{M}_y(t_n)}{I_y} + \hat{\alpha}_{d,\theta}^+(t_n)\right]\Delta$$

$$\hat{\omega}_\psi(t_{n+1}) = \hat{\omega}_\psi^+(t_n) + \left[\frac{I_x - I_y}{I_z}\hat{\omega}_\phi^+(t_n)\hat{\omega}_\theta^+(t_n) + \frac{\hat{M}_z(t_n)}{I_z} + \hat{\alpha}_{d,\psi}^+(t_n)\right]\Delta \tag{8}$$

where I_x, I_y, I_z are vehicle moments of inertia about principal axes; $M_x, M_y, \hat{M}_z$ are commanded jet torques and $\hat{\alpha}_{d,\phi}$, $\hat{\alpha}_{d,\theta}$, $\hat{\alpha}_{d,\psi}$ are estimates of roll, pitch, and yaw disturbing angular accelerations caused by jet failures. The jet failure torques are modeled as Brownian motion processes, so between measurements the disturbing angular acceleration estimates are constant

$$\hat{\alpha}_d(t_{n+1}) = \hat{\alpha}_d^+(t_n) \tag{9}$$

The total complement of angular state estimates thus consists of the attitude quaternion $q_{\hat{B}}^I$, the angular velocity $\hat{\omega}$ and the angular disturbing acceleration $\hat{\alpha}_d$.

Since the three vehicle principal axis moments of inertia are unequal, it follows from Eq. (8) that there will be cross-coupling between the three rotational axes and hence correlation between roll, pitch, and yaw estimation errors. The extended Kalman filter for this angular system would thus have a (9×9) covariance matrix.[11,14] The computational complexity of such an estimator is unwarranted in view of the marginal gain in accuracy that might be obtained by carrying along the correlations between axes. Therefore, it is assumed that there is zero correlation between the roll, pitch, and yaw estimation errors.

Covariance matrix propagation is consistent with the standard extended Kalman filter techniques, except for the elimination of any correlation between channels. The (3×3) covariance matrix for each ξ channel, where ξ is a generalized index assuming the symbols ϕ for roll, θ for pitch and ψ for yaw, is propagated independently of the others according to the equation

$$P_\xi(t_{n+1}) = \Phi P_\xi^+(t_n)\Phi^T + S(t_n) \tag{10}$$

The ordering of state variables in each channel is taken as attitude first, rate second and disturbing acceleration third. Thus

$$\Phi = \begin{bmatrix} 1 & \Delta & \Delta^2/2 \\ 0 & 1 & \Delta \\ 0 & 0 & 1 \end{bmatrix} \tag{11}$$

The matrix $S(t_n)$ is diagonal with the (3,3) element chosen empirically to facilitate tracking of disturbing accelerations due to jet failures, the (2,2) element chosen to model attitude disturbances and allowable thrust variations in unfailed jets and the (1,1) element set to zero.

The measurements available to the angular state estimator are attitude quaternions obtained from the IMU gimbal angle readout system. Define $q_{\tilde{B}}^I$ as the IMU measurement. Then the residual quaternion $q_{\tilde{B}}^{\hat{B}}$ given by

$$q_{\tilde{B}}^{\hat{B}} = (q_{\hat{B}}^I)' \, q_{\tilde{B}}^I \tag{12}$$

represents the rotation by which the estimated body frame $\hat{B}$ would have to be rotated to align with the measured body frame $\tilde{B}$. Assuming accurate measurements and estimates, this rotation will be small, and hence the residual quaternion may be approximated as

$$q_{\tilde{B}}^{\hat{B}} = 1 + \tilde{\epsilon}/2;\ \tilde{\epsilon} = [\tilde{\phi}, \tilde{\theta}, \tilde{\psi}]^T \tag{13}$$

The elements of $\tilde{\epsilon}$ are small angle residuals about the x,y,z vehicle principal axes. The discrete Kalman filter measurement incorporation equations for a system consisting of a state x, a state estimate $\hat{x}$ with error covariance P and a linear measurement with additive noise $y = Hx + w$ with noise variance $\overline{w^2} = R$ are given by[15]

$$P^+ = P - PH^T[HP\,H^T + R]^{-1}HP \tag{14}$$

$$\hat{x}^+ = \hat{x} + P^+H^TR^{-1}(y - H\hat{x}) \tag{15}$$

Since the correlation between angular channels is assumed zero in this study, the rate and disturbing acceleration estimate updates are calculated independently for the roll, pitch, and yaw channels. Because these measurement incorporation equations are analogous for each channel, the equations are presented in general form for the ξ channel, where ξ assumes the symbols ϕ, θ, and ψ for the roll, pitch, and yaw channels respectively.

The IMU provides attitude measurements, so the filter measurement matrix is

$$H=[\ 1\ 0\ 0\ ] \tag{16}$$

Applying Eq. (15) and (16) along with the ξ channel measurement residual $\tilde{\xi}$ from Eqs. (12) and (13) yields the measurement incorporation equations for angular velocity and disturbing acceleration at a discrete measurement time

$$\hat{\omega}_\xi^+ = \hat{\omega}_\xi + P_\xi^+(1,2)\,\tilde{\xi}/r \tag{17}$$

$$\hat{\alpha}_{d,\xi}^+ = \hat{\alpha}_{d,\xi} + P_\xi^+(1,3)\,\tilde{\xi}/r \tag{18}$$

In Eqs. (17) and (18) r is the variance of the measurement error, $P_\xi^+(1,2)$ is the correlation between ξ attitude and rate estimation errors after the measurement, and $P_\xi^+(1,3)$ is the correlation between ξ attitude and disturbing acceleration estimation errors after the measurement. These correlations are elements of the ξ channel covariance matrix defined in terms of its elements as

$$P_\xi = \{P_\xi(i,j)\} \quad i,j=1,2,3 \tag{19}$$

The elements of P_ξ^+ are computed using Eqs. (14) and (16) prior to performing Eqs. (17) and (18).

Measurements are incorporated into the attitude quaternion under the assumption that the total angular correction is small. From Eqs. (15) and (16), the estimated vehicle orientation is updated by rotations of $P_\phi^+(1,1)\tilde{\phi}/r$ in roll, $P_\theta^+(1,1)\tilde{\theta}/r$ in pitch, and $P_\psi^+(1,1)\tilde{\psi}/r$ in yaw. This is accomplished by the following quaternion multiplication. Define

$$q_{\hat{B}_+}^{\hat{B}} = (1 - s\cdot s)^{1/2} + s \tag{20}$$

$$s = [P_\phi^+(1,1)\tilde{\phi}/r,\ P_\theta^+(1,1)\tilde{\theta}/r,\ P_\psi^+(1,1)\tilde{\psi}/r]^T/2 \tag{21}$$

Then from Eq. (6) the updated quaternion estimate is

$$q_{\hat{B}}^I = q_{\hat{B}}^I\ q_{\hat{B}_+}^{\hat{B}} \tag{22}$$

The gimbal angle readout mechanism is not able to determine gimbal angle below a specified granularity or quantum size Q. The best knowledge of the actual gimbal angle is that it lies within $\pm Q/2$ of the gimbal angle output reading. The philosophy of this study is that a quantized measurement of attitude should be incorporated into the attitude state estimates, with a corresponding decrease in the attitude error covariance matrix, only if the measurement adds new information, i.e., only if the measurement is *inconsistent* with the present attitude estimate. The measured quaternion stipulates that the attitude estimation error for the ξ channel ($\xi=\phi,\theta,\psi$) must be in the interval

$$[\ \tilde{\xi} - Q/2,\ \tilde{\xi} + Q/2\ ] \tag{23}$$

while the ξ channel state estimator is interpreted as contending that the attitude estimation error is zero. Thus the attitude quaternion measurement is incorporated into the ξ channel estimate if the region given by Eq. (23) does not include zero, i.e., if

$$|\tilde{\xi}| > Q/2 \tag{24}$$

If Eq. (24) is satisfied, the measurement is incorporated into the ξ channel. The measurement noise is $r=Q^2/12$, the variance for a uniform distribution of width Q.

It may occur that for one or more channels the estimate and measurements will be consistent over many samples, and no measurement incorporations will occur. As a result, the filter covariance will grow via Eq. (10), and the angular position error covariance may, unrealistically, become larger than r. Therefore, at each sample time, if Eq. (24) is not satisfied and if $P_\xi(1,1) > r$, a covariance shaping is accomplished by performing Eq. (14) for the ξ channel without changing the ξ channel estimates.

To summarize the rotational state estimator, at each sample time the roll, pitch, and yaw residuals are calculated using Eqs. (12) and (13). If the residual $\tilde{\xi}$ satisfies Eq. (24), Eqs. (14), (17), and (18) are performed for the ξ channel, and $\tilde{\xi}$ is inserted into Eq. (21). If the residual $\tilde{\xi}$ does not satisfy Eq. (24), $\tilde{\xi}=0$ is inserted into Eq. (21) and if $P_\xi(1,1) > r$, Eq. (14) is performed for the ξ channel. After these steps have been carried out for all three attitude channels, i.e., for $\xi=\phi,\theta$, and ψ, then Eqs. (20) and (22) are performed. Between sample times, the roll, pitch and yaw covariances are propagated using Eqs. (10) and (11) for $\xi=\phi,\theta$, and ψ, and the state estimates are propagated using Eqs. (7-9).

Translational Estimation

The difference between the output of an inertially stabilized IMU's integrating accelerometer from one time to another is a measure of the integral of one component of specific force applied to the vehicle over that time interval. The change in the integral can be written as

$$v_i(t_\ell) - v_i(t_k) = \int_{t_k}^{t_\ell} [R_{B,i}^I(a_d + a_j) + \eta_i]\,dt \tag{25}$$

where explicit time dependence of the variables is dropped for notational convenience. $R_{B,i}^I$ is the ith row of the direction cosine matrix transforming principal body axes to IMU inertial axes.† a_d is the disturing linear acceleration in body coordinates, assumed constant between times t_k and t_ℓ. a_J is the acceleration due to commanded jet firings, assumed constant between successive sample times t_n and t_{n+1}. η_i is the process noise acceleration caused by crew motion, machinery, etc., also assumed constant between successive sample times.

The output of the ith accelerometer at time t_j is given by

$$m_i(t_j) = Q\{v_i(t_j) + \int_{t_0}^{t_j} b_i dt\} \tag{26}$$

where $Q\{\cdot\}$ denotes quantization of the quantity in brackets and b_i is the instrument bias in the ith accelerometer, assumed constant. The measurement shown in Eq. (26) can be written as the sum of the quantity in brackets and an error term. This error term is defined to consist of a mean value and a random component. Thus Eq. (26) becomes

$$m_i(t_j) = v_i(t_j) + \int_{t_0}^{t_j} b_i dt + \bar{e}_{m,i}(t_j) + \mu_i(t_j) \tag{27}$$

where $\bar{e}_{m,i}(t_j)$ is the mean value of the quantization error at t_j and $\mu_i(t_j)$ is the random component of the quantization error at t_j. The values of these quantities depend upon the acceleration level at the time of the measurement and the value of the measurement one sample previously, and are discussed in Appendix A.

Since the actual values of a_J and b_i are not known, they may be written as the sum of their a priori means and random errors as

$$a_J = \bar{a}_J + e_J;\quad b_i = \bar{b}_i + e_{b,i} \tag{28}$$

†The transformation matrix R_B^I is easily calculated from the attitude quaternion q_B^I.[12]

where $\bar{b}_i$, the calibrated bias, and $e_{b,i}$, the uncalibrated bias, are constant. Substituting Eqs. (27) and (28) into Eq. (25) and rearranging gives

$$m_i(t_\ell) - m_i(t_k) - \bar{e}_{m,i}(t_\ell) + \bar{e}_{m,i}(t_k) - \int_{t_k}^{t_\ell} (R^I_{B,i}\bar{a}_J + \bar{b}_i)\,dt$$
$$= \int_{t_k}^{t_\ell} R^I_{B,i}\,dt\; a_d + \int_{t_k}^{t_\ell} [R^I_{B,i}e_J + \eta_i + e_{b,i}]\,dt + \mu_i(t_\ell) - \mu_i(t_k) \quad (29)$$

Equation (29) is a key result for the linear disturbing acceleration estimator, and is in the standard from $y = Hx + w$, where a_d is the state to be estimated.

Because the object of this study is the design of a discrete filter, certain assumptions are made regarding the forms of the errors in Eq. (29). In particular, the error e_J and the driving noise η_i are assumed constant over a sample period and uncorrelated from one sample period to another. Using a sample period of Δ, with $t_j \le t < t_{j+1}$, define

$$E_J(t_j) = \overline{e_J(t)e_J(t)^T}\,\Delta^2; \quad E_{b,i} = \overline{e^2_{b,i}}$$
$$E_{\eta,i}(t_j) = \overline{\eta_i(t)^2}\Delta^2; \quad E_{\mu,i}(t_j) = \overline{\mu_i(t_j)^2} \quad (30)$$

Then the covariance of the measurement noise in Eq. (29) is given to first order by

$$W_i(t_\ell,t_k) = \sum_{j=k}^{\ell-1} [R^I_{B,i}(t_j)E_J(t_j)R^I_{B,i}(t_j)^T + E_{\eta,i}(t_j)]$$
$$+ (t_\ell - t_k)^2 E_{b,i} + E_{\mu,i}(t_k) + E_{\mu,i}(t_\ell) \quad (31)$$

Because the estimator is required to follow a step change in the disturbing linear acceleration a_d, arising from a jet leak or hard failure, the filter must postulate the existence of some noise driving a_d between sample times. Thus the covariance of the error in the estimate of a_d, P_d, satisfies the recursive equation

$$P_d(t_{n+1}) = P_d(t_n) + S_d(t_n) \quad (32)$$

where $S_d(t_n)$ is the covariance of the fictitious driving noise. The estimate of the disturbing linear acceleration is held constant over the sample interval, i.e.,

$$\hat{a}_d(t_{n+1}) = \hat{a}^+_d(t_n) \quad (33)$$

Defining the summation of measurement noise in Eq. (31) as $\tilde{E}_i(t_\ell,t_k)$, it follows that the recursive formula for $\tilde{E}_i(t_n,t_k)$ is given by

$$\tilde{E}_i(t_{n+1},t_k) = \tilde{E}(t_n,t_k)$$
$$+ R^I_{B,i}(t_n)E_J(t_n)R^I_{B,i}(t_n)^T + E_{\eta,i}(t_n) \quad (34)$$

Defining the measurement geometry vector as

$$H_i(t_\ell,t_k) = \int_{t_k}^{t_\ell} R^I_{B,i}(t)\,dt \quad (35)$$

it follows that between samples $H_i(t_n,t_k)$ propagates via the approximation

$$H_i(t_{n+1},t_k) = H_i(t_n,t_k) + R^I_{B,i}(t_n)\Delta \quad (36)$$

Also, defining the jet command measurement component as

$$C_i(t_\ell,t_k) = \int_{t_k}^{t_\ell} R^I_{B,i}(t)a_J(t_n)\,dt \quad (37)$$

it follows that between samples $C_i(t_n,t_k)$ propagates via the approximation

$$C_i(t_{n+1},t_k) = C_i(t_n,t_k) + R^I_{B,i}(t_n)a_J(t_n)\Delta \quad (38)$$

Measurement incorporation in the disturbing linear acceleration filter occurs in two different situations. A measurement is incorporated whenever the output of any of the integrating accelerometers changes between samples. This fits well into the linear filter theory since the measurement errors from one measurement interval to another are essentially uncorrelated. In addition, measurements are incorporated when unchanging instrument outputs are inconsistent with the current estimate of the disturbing linear acceleration. These incorporations, called pseudo-measurement incorporations, keep the disturbing acceleration estimate and its covariance consistent with the quantized measurements. They are discussed in Appendix B.

To derive the equations for incorporation caused by output change, assume that at time t_k the value of m_i changes from its value one sample previously, and that m_i remains constant until time t_ℓ, when it changes value again. Over the time interval from t_k to t_ℓ, a change in the ith component of inertial velocity is indicated by the measurements, and this velocity change may be used to update the estimate of the disturbing linear acceleration. The discrete linear measurement update equations are given in Eqs. (14) and (15) for the general scalar measurement case. For this particular problem, it follows from Eqs. (29-31), (35), and (37) that

$$P = P_d(t_\ell);\; H = H_i(t_\ell,t_k);\; R = W_i(t_\ell,t_k);\; \hat{x} = \hat{a}_d(t_\ell);$$
$$y = m_i(t_\ell) - m_i(t_k) - \bar{e}_{m,i}(t_\ell) + \bar{e}_{m,i}(t_k) - C_i(t_\ell,t_k) - (t_\ell - t_k)\bar{b}_i \quad (39)$$

The values of the quantization biases $\bar{e}_{m,i}$ and noises $E_{\mu,i}$ depend on the jet firing activity at times t_k and t_ℓ, and values for these quantities are developed in Appendix A. In particular, if m_i changes values at t_j when no jets are firing, the measured quantity is known to be exactly halfway between $m_i(t_{j-1})$ and $m_i(t_j)$. Thus there is a bias on $m_i(t_j)$ with magnitude $Q_v/2$, and the measurement noise is zero. On the other hand, if jets are firing there is no bias on $m_i(t_j)$, and the noise has covariance $Q_v^2/12$.

III. Soft Jet Failure Identification

The term soft failure is used herein to designate a fuel or oxidizer leak in a vehicle RCS jet. Such failures occur typically when either an oxidizer or fuel valve, but not both, remains open when the associated jet is not being commanded to fire. Since only one valve is open the jet does not fire, but the expulsion of oxidizer or fuel produces a small force on the vehicle, typically of the order of ten pounds. Since the inherent reliability of the jets is quite high, it is tacitly assumed that no more than one jet leak will occur at any time. If a single jet is leaking it produces translational and rotation disturbing accelerations which are linearly related to the thrust produced by the leak. If $\alpha_{d,\phi}, \alpha_{d,\theta}, \alpha_{d,\psi}$ represent angular disturbing accelerations of the vehicle with respect to an inertial reference about the three principal body axes, and $a_{d,x}, a_{d,y}, a_{d,z}$ represent linear disturbing accelerations in the three principal axis directions; then these six accelerations are related, through the geometric and inertia properties of the vehicle, to a leak at the ith jet station as

$$a = \begin{bmatrix} \alpha_d \\ \text{--------} \\ a_d \end{bmatrix} = c_i f_i \quad (40)$$

where f_i = force exerted by a leak at the ith jet station and c_i = six-vector array of influence coefficients relating jet force at the ith station to angular and linear vehicle accelerations.

In Sec. II, estimators were developed which provide near optimal estimates of the rotational and translational disturbing accelerations of the vehicle. Although the estimators are nonlinear, it is reasonable to assume that the probability density of the acceleration estimates, conditioned on the measurement history, is normal. Under this assumption, the probability density for the combined angular and linear disturbing accelerations, conditioned on the measurement history M, is[14]

$$p(a\,|M) = (2\pi)^{-3}\,|P_a|^{-\frac{1}{2}}\exp\{-\tfrac{1}{2}(a-\hat{a})^T P_a^{-1}(a-\hat{a})\} \tag{41}$$

where a is the composite vector of angular and linear disturbing accelerations, $\hat{a}$ is the composite vector of disturbing acceleration estimates and P_a is the estimation error covariance matrix of the disturbing accelerations.

In Sec. II, the translational and rotational estimators were decoupled for the purpose of simplifying the overall estimation problem. Hence the covariance P_a is approximated as a block diagonal matrix, assuming no correlation between translational and rotational estimation errors. Also, since the angular estimation system is further decoupled into separate roll, pitch, and yaw channels, the rotational submatrix is diagonal.‡

Now, the linear and angular acceleration states are linearly related to jet station failures according to Eq. (40). There are a total of fourteen jet stations, each characterized by its influence coefficient vector c_i. A failure at the ith station must produce an acceleration in the c_i direction. At any instant of time, only one of the fourteen stations can exhibit a failure. Based on the measurement history, the maximum likelihood force exerted by a failed jet at the ith station is the value of f_i that maximizes Eq. (41) with $c_i f_i$ substituted for a. This is equivalent to obtaining the minimum of the quadratic form in the exponential in Eq. (41)

$$f_i^* = \arg\{\min_{f_i}[(c_i f_i - \hat{a})^T P_a^{-1}(c_i f_i - \hat{a})]\} \tag{42}$$

and performing the minimization in Eq. (42) yields

$$f_i^* = c_i^T P_a^{-1}\hat{a} / c_i^T P_a^{-1} c_i \tag{43}$$

where, if f_i^* computed via Eq. (43) is negative, it is automatically set to zero.

Equation (43) is used to obtain the maximum likelihood jet force for each of the fourteen jet stations. These values constitute the best fits available, under the constraints imposed by the geometry of the jet station positions and firing directions, to the assumed conditional statistics of the disturbing accelerations.

Given the maximum likelihood jet force estimates f_i^*, the question arises as to how well these values fit the measurement data. Since it is assumed that only one soft failure may have occurred, a choice must be made between the fourteen stations as to which of the fourteen estimates f_i^* best fits the data. This is accomplished by choosing the jet whose estimate maximizes the conditional density function given by Eq. (41) and therefore minimizes the likelihood argument $\ell(f_i^*)$ given by

$$\ell(f_i^*) = (c_i f_i^* - \hat{a})^T P_a^{-1}(c_i f_i^* - \hat{a}) \tag{44}$$

In other words, the index of the most likely jet failure, j, is given by

$$j = \arg\{\min_i \ell(f_i^*)\} \tag{45}$$

‡In the steady-state algorithm, P_a is diagonal with all rotational diagonal elements equal and all translational diagonal elements equal.

Although it is quite important to indicate a jet failure quickly, it is also most important to guard against false alarms and thus ensure a believable FDI system. For this reason a rather conservative sequence of logical decisions is used to determine whether a soft failure has in fact occurred. The decision process utilizes the maximum likelihood estimates and likelihood arguments described above.

Decision points occur every τ sec in time. At a decision point, the translational and rotational disturbing acceleration estimates are used to determine the maximum likelihood estimate f_i^* at each station, according to Eq. (43). Correspondingly, the arguments of the likelihood functions are evaluated for each of the estimates via Eq. (44). The value of $\ell(f_i^*)$ is an indication of how well the estimate f_i^* fits the conditional statistics of the disturbing acceleration state variables. Since the disturbing acceleration a is six-dimensional, a value of $\ell(f_i^*)$ greater than 20 implies that the estimate f_i^* lies outside of the ellipsoid of constant probability density containing 99.7% of the probability mass. If the problem were of single dimension, this would be analogous to a sample value that deviated from the mean by more than three standard deviations.

The first of the decision steps is based on the values of $\ell(f_i^*)$ corresponding to the fourteen most likely jet force estimates. If all fourteen $\ell(f_i^*)$ values exceed 20, it is assumed that none of the estimates fit the data well enough to make a failure decision, and a no-fail indication is given. If, however, one or more of the f_i^* estimates yield a value of $\ell(f_i^*)$ less than 20, these estimates are consistent with the conditional statistics of a and the decision sequence proceeds.

The second step involves a comparison of the smallest likelihood argument with all other arguments. If all other values of $\ell(f_i^*)$ exceed the smallest by more than 6, then the decision sequence proceeds to the next step. If, however, one or more of the $\ell(f_i^*)$ values is within 6 of the smallest value, it is assumed that sufficient ambiguity exists so that no failure decision can be made and a no-fail indication is given. This check is the generalized likelihood ratio test.[10] If two $\ell(f_i^*)$ values differ by 6, then the probability that the actual sample lies within a small region around one estimate is twenty times larger than the probability that the actual sample lies within an identical region around the other estimate.

The third step is a simple magnitude check on the f_i^* estimate with the smallest likelihood argument $\ell(f_i^*)$, i.e., jet station j given by Eq. (45). If the magnitude of the estimate f_j^* is less than 5 lb, no failure is indicated. If the estimate exceeds 5 lb, the size of the most likely leak estimate is considered significant and a leak failure is identified at jet station j.

IV. Hard Jet Failure Identification§

Hard failures are defined as either the event that a jet is firing when it is not commanded to fire or does not fire on command to fire. In either case, the 900 lb force acting on the vehicle in an unprescribed manner produces large disturbances. These disturbances appear quickly and dramatically as large measurement residuals in the translation and rotation state estimators, described in Sec. II. Whereas the detection and identification of soft failures is accomplished as a single decision process, hard failure are dealt with in what amounts to a two-step process. First, the presence of a hard failure is detected and then the hard failure is identified. The hard failure detection logic is a simple conservative check on the magnitudes of the measurement residuals. If the magnitude of any of the six measurement residuals exceeds ten times its standard deviation, the presence of a hard failure is indicated, and the system proceeds to hard failure identification.

The filtering and logic system developed for soft failures is modified and utilized for hard failure identification. Once a

§Vernier jet hard failures produce small forces and are therefore identified using the soft failure logic.

failure has been detected, the filter gains are appreciably increased to facilitate tracking of the large disturbing acceleration. The gain increases correspond to multiplying the standard deviations of the process noise driving the disturbing acceleration states by a factor of 100. In this manner the filter states which estimate the disturbing accelerations are made quite responsive and react quickly to the large measurement residuals.

The remainder of the hard failure identification method is nearly identical to the soft failure method, described in Sec. III. The jet force magnitude check level is increased to 100 lb to reflect the fact that the hard failure magnitude is 900 lb rather than the 10 lb level assumed for soft failures. Additionally, negative values for the force estimates f_i^* are allowed, and correspond to off-type jet failures.

V. Simulation Results

The FDI system developed in the previous sections was tested by accurate simulation of the rigid body dynamics of the space shuttle orbiter vehcile. Both the estimator sample period and the FDI system decision periods were chosen to be 0.2 sec. Initially the complete FDI system, as described above including real time estimation error covariance calculations, was employed, and the results were most encouraging. Although this system exhibited fast and accurate FDI, the real time covariance propagation would impose a rather severe computational burden on a flight computer. Careful scrutiny of time histories of the estimation error covariances indicated that they did not vary appreciably during a typical simulation run and stayed relatively constant from run to run. Hence it appeared feasible to use constant error covariance values in the FDI system, thereby eliminating the need for real time error covariance matrix computations.

As a result of this finding, a constant covariance version of the FDI system was developed. Error covariance values obtained from the real time simulations were stored and utilized to determine estimator gains, as described in Sec. II, and for the likelihood function computations of Sec. III. All operations such as the residual traps, measurement covariance calculations for the translational channel and estimator gain calculations, as developed in Sec. II, were retained except that prestored constant values for the estimation error covariances were used in place of real time calculated values. (Appendix C contains some additional logic required to guarantee stability in the translational state estimator.) The results reported in the following sections were obtained with this constant error covariance version of the FDI system.

A considerable body of simulation results has been amassed in order to evaluate overall system performance for a variety of situations. Soft failures were simulated for a variety of conditions involving jet firings for high and low rate attitude maneuvers, crew and machinery motion, accelerometer biases, gravity gradient torques and various orientations of the vehicle relative to the IMU. It was found that jet leaks, producing 10 lb of force, were identified in less than 70 sec, and no missed alarms or false alarms were encountered in any of the simulations. Hard failures were identified in less than 2 sec.

The simulator provided an accurate six degree of freedom rigid body model of the vehicle rotation and translation dynamics, using mass and inertia properties for the 140C shuttle orbiter design. Random disturbances corresponding to foreces in the x,y, and z directions of 5 lb rms, applied at the cockpit for 0.2 sec intervals and uncorrelated between intervals, were used to model crew and machinery motion within the vehicle. When jets were firing normally, they had nominal thrust levels of 900 lb with random deviations of 50 lb rms. The inertial instruments quantized angle and velocity measurements to 20 sec and 1 cm/respectively. Accelerometer biases of 50μ g rms were used, and it was assumed that there was uncertainty of 3μ g rms in knowledge of these biases. This

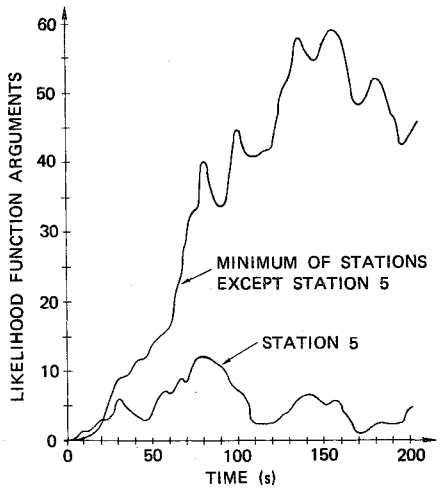

Fig. 2 Likelihood function arguments.

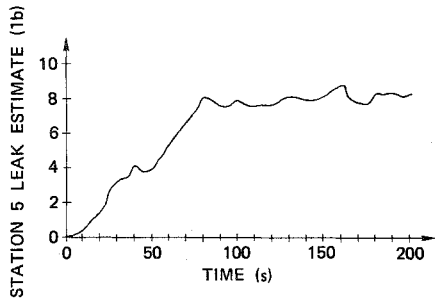

Fig. 3 Maximum likelihood estimate of station 5 thrust.

uncertainty is consistent with an accelerometer bias calibration interval of 2 min.

As described above, the state estimation error covariance values used by the FDI system were constants chosen from the real time covariance calculation simulations performed previously. The estimator design was based on parameter values for the various process noises which were assumed as inputs to the estimated state variables. At the acceleration level, the process noise strength was chosen equivalent to independent white noises of strength 5×10^{-3} lb^2/sec, applied at each of the 14 jet stations. This process noise was intended to make the acceleration estimator states responsive to jumps in jet thrust level representing jet leaks and was chosen empirically from simulations to obtain good estimator performance. On the detection of a hard primary jet failure, this noise strength was increased to 50 lb^2/sec to facilitate rapid estimation of the large disturbing accelerations. At the velocity level, noise input with strength 5 lb^2 sec, equivalent to the crew and machinery motion noise used in the simulator, was used. When a jet was firing, the noise strength at the velocity level was increased to 2000 lb^2 sec to represent the uncertainty in thrust level for a firing jet. Finally, to account for uncertainty in the accelerometer biases, the translational estimator employed a bias error variance of $9(\mu g)^2$.

Because of the dissimilar effects of the fourteen jet station process noises described previously on each of the three linear and three angular channels, the resulting (2,2) and (3,3) elements of S for the roll, pitch, and yaw channels and the diagonal elements of S_d were all different for the real time covariance calculations. Thus, the estimation error covariances for the roll, pitch, and yaw channels were all different, as were the diagonal elements of the linear disturbing acceleration estimation error covariance. Identical constant gains and disturbing angular acceleration error variances for the three angular channels were obtained by averaging over all three channels and many measurement incorporations. A similar method was used to obtain identical disturbing linear

Table 1 Process noise variances used in real time covariance calculations

Variable	Units	Condition I	Condition 2	Condition 3
$S_\phi(2,2)$	rad^2/sec^2	5.92×10^{-11}	6.52×10^{-8}	6.52×10^{-8}
$S_\phi(3,3)$	rad^2/sec^4	6.56×10^{-13}	6.56×10^{-13}	8.05×10^{-8}
$S_\theta(2,2)$	rad^2/sec^2	5.37×10^{-11}	3.36×10^{-8}	3.36×10^{-8}
$S_\theta(3,3)$	rad^2/sec^4	3.01×10^{-13}	3.01×10^{-13}	2.49×10^{-8}
$S_\psi(2,2)$	rad^2/sec^2	5.13×10^{-11}	3.12×10^{-8}	3.12×10^{-8}
$S_\psi(3,3)$	rad^2/sec^4	2.79×10^{-13}	2.79×10^{-13}	3.55×10^{-8}
$S_d(1,1)$	ft^2/sec^4	5.2×10^{-11}	5.2×10^{-11}	6.49×10^{-6}
$S_d(2,2)$	ft^2/sec^4	8.51×10^{-11}	8.51×10^{-11}	3.61×10^{-5}
$S_d(3,3)$	ft^2/sec^4	1.04×10^{-10}	1.04×10^{-10}	2.08×10^{-5}

Table 2 Parameter values used in simulation

$I_x = 8.67\times10^5$ slug ft^2
$I_y = 6.82\times10^6$ slug ft^2
$I_z = 6.98\times10^6$ slug ft^2
Vehicle weight $= 2.45\times10^5$ lb
$Q = 9.70\times10^5$ lb
$Q_v = 0.0328$ ft/sec
$E_b = 10^{-8}$ ft^2/sec^4
$E_n = 1.72\times10^{-8}$ ft^2/sec^2

$$E_j = \begin{cases} 6.88\times10^{-6}\ \text{ft}^2/\text{sec}^2 & \text{with jet firing} \\ 0 & \text{with no jet firing} \end{cases}$$

acceleration error variances for the three linear translation channels. Three sets of constant gains and disturbing acceleration estimation error covariances were found to be sufficient. One set was used for each of the following conditions: 1) no hard failure detected and no jets firing, 2) no hard failure detected and some jet firings, and 3) hard failure detected. The numerical values of the three sets of constant gains and variances are given in Ref. 16. Table 1 shows the nonzero elements of the process noise covariances used in the real time covariance calculations mentioned above. Table 2 indicates some additional parameter values used in the simulation.

In order to lend insight into the performance of the FDI system, a particular simulation run will be discussed in some detail below. In this test case a leak at station 5 occurs after a jet at that station has fired for 2 sec. At the beginning of the firing there is no vehicle angular velocity. The jet fires normally for the 2 sec period, but when commanded to cease firing either a fuel or oxidizer valve stays open and produces a 10 lb force on the vehicle. The 10 lb leak persists for the remainder of the simulation. Unfailed jets are commanded to fire for 2 sec intervals every 40 sec in order to test the FDI system's ability to detect leaks in the presence of jet activity.

Figure 2 shows the evolution of the likelihood argument for station 5. Also plotted is the minimum, at each point in time, of the likelihood function arguments for the other 13 stations. As can be seen, after approximately 20 sec the station 5 likelihood function argument is the smallest and stays below 20 during the entire run. At about 38 sec all other arguments exceed the station 5 argument by more than 6, and this spread is exceeded for the remainder of the run. Figure 3 depicts the evolution of the likelihood estimate of the station 5 jet thrust. The level increases gradually and approaches the true force level of 10 lb at about 270 sec. The 5 lb threshold crossing, required for failure identification, occurs at 57 sec, at which point a leak failure warning is issued.

This particular case is quite typical of the performance of the FDI system. As mentioned above, the FDI logic is quite conservative and therefore guards against false alarms. This conservative logic tends to delay identification somewhat, but provides a highly reliable, believable system. For simulated leaks at other stations, identification times of the order of one minute were attained, with a minimum time of 28.2 sec and a maximum of 68.6 sec.

A number of additional results were apparent from detailed examination of the simulation data. If a jet firing occurs after a leak has begun but before identification, the estimator effectively ignores measurement information during the firing, and identification is delayed. Also, it was found that identification occurs faster if there is a known bias on the accelerometers. By the very nature of quantized measurements, much more information is available when pulses are output from the instrument than when no pulses are available. The presence of a known accelerometer bias assures the output of pulses, even when there is no jet activity, thereby ensuring a high information rate to the FDI system and better identification performance.

Simulation of primary jet hard failures yielded results qualitatively similar to the soft failure results reported above. Detection times of the order of 0.5 sec were obtained with maximum detection times of 0.6 sec, while identification times of the order of 1.5 sec were obtained with a maximum value of 1.6 sec. As with the soft failure detection system, no hard failure false alarms or missed alarms were encountered in any of the simulations.

By employing the estimators during a one or two minute calibration period at the beginning of the orbital mission phase to calibrate the Euler coefficients in Eq. (8), of the form $(I_i - I_j)/I_k$, and the accelerometer biases $\bar{b}_i$; the FDI system was made relatively insensitive to off-nominal parameter values. In addition, the simulation also indicated that the FDI algorithm performed well over a wide range of vehicle angular velocities.

VII. Conclusions

An effective software RCS FDI system has been developed for the orbital phase of the space shuttle mission. The method uses only measurements available from the IMU. In addition to its FDI function, the system also provides accurate vehicle attitude and angular velocity estimates for use by the attitude control system. The FDI system is effective in detecting and identifying both leaks and hard jet failures. Typically primary jet leaks and vernier jet hard failures are identified within approximately 70 sec, and primary jet hard failure detection requires 0.6 sec with identification within an additional second. Performance of the system has been proven by simulation, and no false alarms or missed alarms were encountered.

Appendix A: Quantization Bias and Random Noise

The integrating accelerometers on the shuttle orbiter IMU's are assumed to have the standard staircase input-output structure. Thus, a single quantized measurement of the ith component of velocity at time $t_n, m_i(t_n)$, gives an unbiased measurement of the input with a measurement error uniformly distributed $\pm Q_v/2$ about the measurement, where Q_v is the linear velocity quantum size. The covariance of such a uniform distribution is easily calculated to be $Q_v{}^2/12$. Thus, defining the bias of the quantized measurement to be $\bar{e}_{m,i}(t_n)$ and the covariance of the measurement error to be $E_{\mu,i}(t_n)$, it follows that for a single quantized measurement $m_i(t_n)$

$$\bar{e}_{m,i}(t_n) = 0; \quad E_{\mu,i}(t_n) = Q_v{}^2/12 \tag{A1}$$

Table A1 Output change measurement incorporation summary

Jet firing between times t_{k-1} and t_k?	Jet firing between times $t_{\ell-1}$ and t_ℓ?	Equation applicable at time t_k $(n=k)$	Equation applicable at time t_ℓ $(n=\ell)$
Yes	Yes	A-1	A-1
Yes	No	A-1	A-2
No	Yes	A-2	A-1
No	No	A-2	A-2

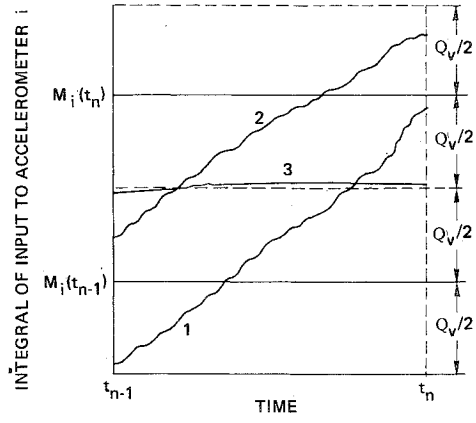

Fig. A1 Possible accelerometer input integral given an output change.

Now, consider a system which samples the quantized measurements discretely. Assume that at time t_{n-1} the accelerometer output has the value $m_i(t_{n-1})$, and that at time t_n the accelerometer output changes one quantum level to $m_i(t_n)$. This situation is shown in Fig. A-1.

At time t_{n-1}, the actual velocity must be in the region $\pm Q_v/2$ about $m_i(t_{n-1})$, while at time t_n the actual velocity must be in the region $\pm Q_v/2$ about $m_i(t_n)$. If a jet is firing between times t_{n-1} and t_n large accelerations are present, and any of the three trajectories shown is possible. Thus $m_i(t_n)$ must be considered an unbiased measurement, and the measurement bias and covariance are given by Eq. (A1). However if no jet is firing in the interval, only small accelerations arising from jet leaks and process noise are present, and only a shallow trajectory such as 3 is possible. In that case, neglecting any small accelerations, the input to the accelerometer is midway between $m_i(t_{n-1})$ and $m_i(t_n)$. Thus $m_i(t_n)$ is essentially a perfect biased measurement of the input, and the measurement bias and covariance are approximated as

$$\bar{e}_{m,i}(t_n) = \text{sign}\,[m_i(t_n) - m_i(t_{n-1})]\,Q_v/2$$

$$E_{\mu,i}(t_n) = 0 \tag{A2}$$

Using this information, the measurement bias and covariance approximations for an output change measurement incorporation follow directly. Denoting the time of the previous output change as t_k and the time of the current output change as t_ℓ, the measurement biases and covariances are determined by the firing activity in the intervals just preceding times t_k and t_ℓ. The four possible situations are summarized in Table A1.

Appendix B: Pseudomeasurement Incorporation

The pseudomeasurement incorporation is used to alter the disturbing linear acceleration estimate and/or its covariance to reflect the knowledge inherent in an unchanging quantized velocity measurement. There are two types of pseudomeasurements, defined by the presence or absence of jet activity in the time interval just prior to the last output change of accelerometer i at time t_k.

In the one-sided pseudomeasurement case, there is no jet firing between times t_{k-1} and t_k. Thus, neglecting the effect of disturbing acceleration and process noise over the sample period, $m_i(t_n)$ is a perfect biased measurement of the input, and its bias and covariance are given by Eq. (A2). The fact that the accelerometer output has not changed implies that the change in the accelerometer input is in the interval given by

$$(0, Q_v \text{sign}\,[m_i(t_k) - m_i(t_{k-1})]) \tag{B1}$$

Thus the pseudomeasurement at time t_ℓ, $m_i(t_\ell)$, is unbiased and has variance $Q_v^2/12$ as given by Eq. (A1). The estimated change in the accelerometer input is given by

$$\delta\hat{v}_i = H_i(t_\ell, t_k)\hat{a}_d(t_\ell) + (t_\ell - t_k)\bar{b}_i + C_i(t_\ell, t_k) \tag{B2}$$

If the estimated velocity change given by Eq. (B2) is outside the interval given by Eq. (B1) for a one-sided pseudomeasurement, the estimated disturbing linear acceleration is not consistent with the unchanging accelerometer output, and a pseudomeasurement incorporation is made by performing Eqs. (14) and (15) using the identities given by Eq. (39), where the measurement y may be written as

$$y = \text{sign}\,[m_i(t_k) - m_i(t_{k-1})]\,Q_v/2 - C_i(t_\ell, t_k) - (t_\ell - t_k)\bar{b}_i \tag{B3}$$

In the two-sided pseudomeasurement case, there is a jet firing between times t_{k-1} and t_k. Thus $m_i(t_k)$ is an unbiased measurement of the input, and Eq. (A1) applies. The fact that the accelerometer output has not changed implies that the change in the accelerometer input is in the interval given by

$$(-Q_v, +Q_v) \tag{B4}$$

Again, the pseudomeasurement $m_i(t_\ell)$ is unbiased, and Eq. (A1) applies. If the estimated velocity change given by Eq. (B2) is outside the interval given by Eq. (B4) for a two-sided pseudomeasurement, the estimated disturbing linear acceleration is not consistent with the unchanging accelerometer output, and a two-sided pseudomeasurement incorporation is made by performing Eqs. (14) and (15) using the identities given by Eq. (39), where y may be written as

$$y = -C_i(t_\ell, t_k) - (t_\ell - t_k)\bar{b}_i \tag{B5}$$

In addition to performing one- and two-sided pseudomeasurement incorporations which change both the estimate of the disturbing linear acceleration and its covariance, pseudomeasurement covariance shaping is also employed in the translational estimator to keep the velocity uncertainty from growing larger than the variance of the quantized measurements. This is analogous to the covariance shaping in the rotational state estimator. In particular, an unchanging accelerometer output is always interpreted as indicating that the change in the accelerometer input since the last output change must lie in the interval given by Eq. (B4). The covariance for a uniform distribution over this interval is $Q_v^2/3$, and a covariance shaping is performed if the covariance of the estimated change in accelerometer input is larger than this value. This condition may be written

$$H_i(t_\ell, t_k)P_d(t_k)H_i(t_\ell, t_k)^T + \tilde{E}_i(t_\ell, t_k) + (t_\ell - t_k)^2 E_{b,i} > Q_v^2/3 \tag{B6}$$

At a sample time t_ℓ, if no output change or pseudomeasurement incorporation is made for accelerometer i and Eq. (B6) is satisfied, a pseudomeasurement covariance shaping is made by performing Eq. (14) using the identities

$$P=P_d(t_\ell);\ H=H_i(t_\ell,t_k);\ R=\tilde{E}_i(t_\ell,t_k) + (t_\ell-t_k)^2E_{b,i}+Q_v{}^2/3 \tag{B7}$$

Naturally, covariance shaping is not performed in the constant covariance steady-state filter.

Appendix C: Instability Protection in the Translational Estimator

The translational disturbing acceleration estimator employs a measurement vector [Eq. (36)] that may grow in an unbounded way with time. This technique is necessary to properly process the available measurements when the spacecraft is in a quiescent state and there are long intervals between accelerometer output pulses. However, the use of a constant covariance matrix, as described in Sec. V, is inconsistent with an H vector that can grow large with time. In particular the estimator may become unstable if there are long intervals between accelerometer pulses.

The estimator assumes that P^+ is constant and diagonal with equal diagonal elements ρ^+. Also, the measurement matrix is a row vector so Eq. (15), with the identifications from Eqs. (33) and (39), becomes

$$\hat{x}^+(t_\ell)=[I-\frac{\rho^+}{R}H^TH]\hat{x}^+(t_k)+\frac{\rho^+}{R}H^Ty(t_\ell);\ k<\ell \tag{C1}$$

Since H is a row vector, H^TH has only one nonzero eigenvalue given by

$$\text{eigenvalue}\ \{H^TH\}=HH^T \tag{C2}$$

Uniform stability of Eq. (C1) is guaranteed if

$$\frac{\rho^+}{R}HH^T\leq 2 \tag{C3}$$

and simulation experience has shown that unsatisfactory filter operation is obtained whenever H becomes so large that the bound in Eq. (C3) is approached.

The source of the problem is the inconsistency between the assumption of a constant P^+ and an H vector that can grow without bound. In fact, a true optimal estimator exhibits a much tighter bound than Eq. (C3). Applying the matrix inversion lemma[15] to Eq. (14) yields

$$P^+H^TR^{-1}H=PH^T(HPH^T+R)^{-1}H \tag{C4}$$

Premultiplying by H, postmultiplying by H^T and substituting $P^+=\rho^+I$ yields

$$\frac{\rho^+}{R}(HH^T)^2=\frac{HPH^THH^T}{HPH^T+R} \tag{C5}$$

and since $HH^T<0$ and $R<0$

$$\frac{\rho^+}{R}HH^T=\frac{HPH^T}{HPH^T+R}<1 \tag{C6}$$

which reduces the bound in Eq. (C3) by half.

To ensure that this restriction is met in the translational estimator, Eq. (C6) is checked before a measurement incorporation is made. If Eq. (C6) is not satisfied, the following equation is used in place of Eq. (15)

$$\hat{x}^+=\hat{x}+\frac{H^T}{HH^T}(y-H\hat{x}) \tag{C7}$$

With the restriction of Eq. (C7) the estimator is guaranteed to be uniformly stable. Bounded input/bounded output stability would be guaranteed if it could be assured that over all intervals of a given length T there are sufficient measurements to guarantee that the associated H^T vectors span the three-dimensional state space. In this event the system is stochastically controllable and observable[11] and Liapunov stability follows. In practice it was found that imposing the restriction of Eq. (C7) yields good filter performance with no oscillatory tendencies.

References

[1] Beard, R. V., "Failure Accomodation in Linear Systems Through Self-Reorganization," MVT-71-1, Feb. 1971, Man Vehicle Laboratory, M.I.T., Cambridge, Mass.

[2] Jones, H. L., "Failure Detection in Linear Systems," Ph.D. Thesis, Sept. 1973, Department of Aeronautics and Astronautics, M.I.T., Cambridge, Mass.

[3] Chien, T. T., "An Adaptive Technique for a Redundant Navigation System," T-560, Feb. 1972, Charles Stark Draper Lab., Cambridge, Mass.

[4] Wald, A., *Sequential Analysis*, Wiley, New York, 1947.

[5] Willsky, A. S., Deyst, J. J., Jr., and Crawford, B. S., "Adaptive Filtering and Self-Test Methods for Failure Detection and compensation," Proc. of the 1974 JACC, Austin, Texas, June 19-21, 1974; also submitted to the *AIAA Journal*.

[6] Buxbaum, P. J. and Haddad, R. A., "Recursive Optimal Estimation for a Class of Nongaussian Processes," *Proceedings of the Symposium on Computer Processing in Communications*, Polytechnic Institute of Brooklyn, April 8-10, 1969.

[7] Mehra, R. K. and Peschon, J., "An Innovations Approach to Fault Detection and Diagnosis in Dynamic Systems," *Automatica*, Vol. 7, pp. 637-640.

[8] Willsky, A. S., and Jones, H. L., "A Generalized Likelihood Ratio Approach to State Estimation in Linear Systems Subject to Abrupt Changes," Paper FP4-3, *Proceedings of the 1974 IEEE Conference on Decision and Control*, Phoenix, Arizona, November 20-22, 1974.

[9] Deyst, J. J. and Deckert, J. C., Shuttle Orbiter Reaction Control Subsystem Jet Failure Detection Using a Generalized Likelihood Ratio Technique, R-848, Nov. 1974, The Charles Stark Draper Lab., Cambridge, Mass.

[10] Van Trees, H. L., *Detection, Estimation and Modulation Theory*, Part I, Wiley, New York, 1968.

[11] Jazwinski, A. H., *Stochastic Processes and Filtering Theory*, Academic Press, New York, 1970.

[12] McKern, R. A., "A Study of Transformation Algorithms for Use in a Digital Computer," T-493, Jan. 1968, The Charles Stark Draper Lab., Cambridge, Mass.

[13] Halfman, R. L., *Dynamics*, Vol. 1, Addison-Wesley, Reading, Mass., 1962.

[14] Gelb, Arthur, et al., *Applied Optimal Estimation*, MIT Press, Cambridge, Mass., 1974.

[15] Bryson, A. E. and Ho, Y.-C., *Applied Optimal Control*, Blaisdell, Waltham, Mass. 1969.

[16] Deyst, J. J. and Deckert, J. C., "RCS Jet Failure Identification for the Space Shuttle," Paper 28.2, *Proceedings of IFAC 6th Triennial World Congress*, Boston, Mass., Aug. 1974.